processes

MDPI

Article

Modified Model and Simulation Verification of Rock-Fatigue Damage Considering Repeated Discharge Impact

Jianchun Guo [1,*], Xinyang Li [1], Cong Lu [1,*], Xinlei Zhu [2], Kun Huang [2] and Shiqian Xu [1]

[1] State Key Laboratory of Oil and Gas Reservoir Geology and Exploitation, Southwest Petroleum University, Chengdu 610500, China; zakisoze@163.com (X.L.); shiqianxu@swpu.edu.cn (S.X.)
[2] Tsinghua Sichuan Energy Internet Research Institute, Chengdu 610500, China; ibelieve112358@126.com (X.Z.); huangkun@tsinghua-eiri.org (K.H.)
* Correspondence: guojianchun@vip.163.com (J.G.); lucong@swpu.edu.cn (C.L.)

Abstract: The existing rock-fatigue-damage constitutive model fails to consider the influence of discharge energy and discharge times on the effect of rock damage under discharge impact. In this regard, the impact load test of sandstone was carried out. Based on the test results, the quantitative characterization formula of different discharge parameters on the weakening degree of rock compressive strength was established. Based on the TCK (Taylor–Chen–Kuszmaul) model, a constitutive model considering the mechanical properties of rock and the dynamic hange of micro-crack geometric size is established, and the cohesive model is proposed to calculate the crack size. The constitutive model includes the relationship between crack width, crack number, and rock compressive strength, and the change of damage factor D is used to consider the fatigue-damage effect of discharge shock on the rock. The results show that the modified model can quantitatively and accurately reflect the dynamic damage and failure process of rock and that the weakening of rock mechanical properties and the development of micro-cracks can be controlled by designing different discharge parameters.

Keywords: discharge shock wave; fatigue damage; modify the model; numerical simulation; micro-crack

Citation: Guo, J.; Li, X.; Lu, C.; Zhu, X.; Huang, K.; Xu, S. Modified Model and Simulation Verification of Rock-Fatigue Damage Considering Repeated Discharge Impact. *Processes* **2023**, *11*, 2366. https://doi.org/10.3390/pr11082366

Academic Editors: Qingbang Meng and Yidong Cai

Received: 23 May 2023
Revised: 12 July 2023
Accepted: 31 July 2023
Published: 6 August 2023

1. Introduction

With the increase in global energy utilization, oil and gas extraction has also shifted from conventional to unconventional. Unconventional energy can be defined as reservoir resources that cannot be economically effectively recovered without implementing special stimulation measures. Existing stimulation technologies include fracking, acid fracturing, supercritical CO_2 fracturing, and discharge shock waves [1–3].

Discharge shock waves are a relatively new reservoir modification technology that releases a large amount of stored electrical energy in a short period of time, exerting pressure on the reservoir rocks along the water medium, causing micro-cracks and extending the original cracks in the reservoir rock near the wellbore area.

Repeated action of discharge shock wave will cause fatigue damage to the rock. When rocks are subjected to impact, the strain or stress accumulates until damage occurs, which manifests in the form of micro-cracks. With the continuous increase of the damage degree of the body, the irreversible deformation of the rock will continue to accumulate, and in this process, rock defects such as micro-cracks will also continue to generate and develop, eventually lead to the reduce of the rock strength and failure. Therefore, it can be considered that the development state of micro-cracks characterizes the damage and failure behavior of rocks under the repeated action of the shock wave. Therefore, to explore the fatigue characteristics of rock under the action of the discharge shock wave, it is particularly important to analyze the development state of micro-cracks in the rocks under load.

The fatigue damage of rock under repeated impact is mainly affected by factors such as shock wave load parameters [4–8]. In recent years, many efforts have been made to investigate the fracture behaviors of rock under cyclic loading. For instance, Xiurun found

that the upper-limit stress and amplitude are the main factors that influence the fatigue life of sandstone [9]. Zhou studied the effect of frequency on the mechanical properties of sandstone subjected to cyclic loading, and found that as the frequency increases, the mechanical properties will increase at first and then decrease [10]. Song studied the fatigue behavior of rock materials under multi-stage repeated impact loads and proved that the failure mode and crack size are directly related to the loading mode [11,12].

The mechanical behaviors and evolution characteristics of mineral particles at the mesoscale are internal factors leading to the macromechanical properties of rocks [13,14]. In recent years, the effects of various types of defects, such as cracks, beddings, and holes, on the strength, deformation characteristics, and fracture evolution laws of rocks or rock-like materials have been systematically investigated [15–17].

In recent years, numerical simulations have been widely used to investigate the macro- and mesomechanical properties and failure mechanism of rocks. Budiansky analyzed the dispersed crack group in rock and established the corresponding rock fracture damage model [18]. Grady considered that there are a large number of primary cracks obeying the two-parameter Weibull distribution in the rock [19]. Taylor introduced the expressions of the effective bulk modulus and Poisson's ratio of R.J.O, Connel, with the micro-crack density and the expression formula of the fragment size given by the TCK model [20]. Then, many scholars have proposed a variety of damage constitutive models from the perspective of the dynamic fracture of rock [21,22].

Although the damage caused by impact load to rock is considered in the above model, the dynamic state damage caused by repeated action to the interior of intact rock is not considered. This is because, with the hange of impact load parameters, the micro-crack state generated in the rock body is dynamic. However, the theoretical circle has not yet proposed a dynamic damage constitutive model that can reflect its influence on rock mechanical properties and micro-crack changes. At the same time, previous experiments have also proved that the fatigue damage of rock is dynamically affected by discharge impact energy and impact times. In this study, is based on the theory of fracture mechanics and the classical rock dynamic damage constitutive model (TCK model). Firstly, the cohesive force model is introduced, then the weakening formula of rock mechanics is deduced by experimental means, and finally, the modified dynamic damage model of rock is established by combining the above formulas. It is verified by AUTODYN simulation software. The influence of different discharge energy and times on rock compressive strength and micro-crack formation can be quantitatively obtained by the modified model. The establishment of this model enables a more simplified and accurate application for the reformation of sandstone reservoirs under various reservoir conditions. It greatly advances the application of discharge impact technology in the field of oil and gas reservoirs.

2. Existing Rock Damage Constitutive Model

2.1. TCK Model

According to the existing damage models, when the impact load does not exceed the plastic yield limit of the rock, the fatigue damage of the rock is mainly manifested as an elastic-brittle failure caused by micro-crack propagation. Therefore, the evolution of rock fatigue damage is generally determined by the change in rock element micro-crack density.

The TCK model is a dynamic damage constitutive model of rock based on the microscopic damage mechanism. The basic assumption is that rock is the isotropic material, and under the action of external force, the rocks defects will initiate, expand and even connect, leading to its failure [23].

$$\sigma(n) = E(1 - D)\varepsilon(n) \tag{1}$$

where σ is the stress in tensor form (MPa), ε is the volume strain (dimensionless), E is the elastic modulus (MPa), D is the damage variable; n is the number of discharges (dimensionless).

The damage coefficient D caused by micro-cracks is defined by the bulk modulus of the medium as follows:

$$D = 1 - \frac{\overline{K}}{K} \tag{2}$$

Budiamsky and O'Connel proposed an expression for the effective bulk modulus of cracked solids [18].

$$\frac{\overline{K}}{K} = 1 - \frac{16}{9}\frac{(1-\overline{\nu}^2)}{(1-2\overline{\nu})}C_d \tag{3}$$

where $\overline{K}$ is the effective bulk modulus (MPa), K is the original bulk modulus (MPa), $\overline{\nu}$ is the effective Poisson's ratio (dimensionless), C_d is micro-crack density (quantity/cm^2).

The crack density is the ratio of the rock volume in the crack-affected zone to the total rock volume.

$$C_d = \beta N a^3 \tag{4}$$

where β is the coefficient (dimensionless), $\beta = 3$, a is the average radius of micro-cracks (mm), N is the number of cracks activated by rock impact (quantity).

Under volume tension, the number of activated micro-cracks in the rock obeys the Weibull distribution [19].

$$N = k\varepsilon^m \tag{5}$$

where k, m are rock parameters in the damage model (dimensionless), $k = 7.47 \times 10^{15}$, $m = 6$.

Parameter m relates to the ultimate tensile stress and strain rate of rock materials. Grady believed that m is a constant.

The material parameter k is obtained by tensile fracture experiments at different strain rates.

Combined with the above formula, the damage coefficient is related to the crack density, and the damage coefficient is defined as follows:

$$D = \frac{16}{9}\frac{(1-\overline{\nu}^2)}{(1-2\overline{\nu})}\beta N a^3 k\varepsilon^m \tag{6}$$

2.2. Existing Problems

The above rock fatigue damage model treats the dynamic damage of rock under load as a continuous process and defines the damage variable as a function of crack density from the perspective of micromechanics, but the current theoretical model does not consider the dynamic hange of the average micro-crack radius parameter of crack density under the influence of different discharge energy and discharge times during the discharge impact process in practical application.

However, how to describe the effect of different discharge energy and discharge times on the weakening of rock mechanical properties and the formation of micro-cracks is the key and difficult problem in the current study of discharge impact dynamics.

To solve this problem, many scholars have put forward many different methods from different angles. For example, Kyoya defined the damage tensor of rock mass with a set of parallel cracks as follows [24]:

$$\Omega = \frac{l}{V}\sum_{k=1}^{N} a_k(n_k \otimes n_k) \tag{7}$$

where Ω is the damage tensor of jointed rock mass (MPa), l is the average crack spacing (mm), V is the sample volume (mm^3), N is the number of cracks in the sample; a_k is the surface area of the k-th crack in the sample (mm^2), n_k is the unit normal vector on the surface of the k-th crack in the sample (dimensionless).

This is also one of the most commonly used damage tensor calculation methods in rock damage theory, but it also has certain defects. Beceuse this method only considers the effect of micro-crack length and does not consider the effect of crack strength properties, which is

inconsistent with the rock mechanical properties that weaken the compressive strength of rocks under repeated discharge impact. Therefore, Kawamoto modified the above model by introducing crack pressure transfer and shear transfer coefficient to consider how the characteristics of those joints can transfer partial compressive stress and shear stress under compressive loads [25].

$$\Omega = \frac{l}{V^{2/3}} \left[\frac{N_1 N_2 L_1 L_2}{\sqrt{\left[\left(1 - n_1^2\right) \left(1 - n_2^2\right) \right]}} \right]^{1/2} (n \otimes n) \tag{8}$$

It can be seen from the current research that for the fatigue damage constitutive model of rocks, it is generally believed that the joint effects of crack geometry and strength characteristics, such as compressive strength, should be considered simultaneously. However, the current research is still to first define the damage tensor according to the geometric characteristics of the cracks and then modify the above calculation results through the strength characteristics of the cracks, which not only causes inconvenience in the use of the model but also makes the theoretical calculation results difficult to apply to engineering practice due to the randomness of the empirical parameter values.

Based on the previous research on rock damage mechanics, this paper uses experimental methods to establish a calculation method that can obtain the crack geometry and mechanical properties through the hange of discharge energy and discharge parameters based on the action characteristics of the discharge shock wave and improves the correction formula of the TCK model.

3. Model Correction

3.1. Model Improvement Formula

For the average radius of micro-cracks formed by rock damage, Grady's expression is often used [19].

$$a = \frac{1}{2} \left(\frac{\sqrt{20} K_{IC}}{\rho C_p \varepsilon_{\max}} \right)^{\frac{2}{3}} \tag{9}$$

where K_{IC} is fracture toughness (MPa), ρ is density (kg/m^3), C_P is longitudinal wave velocity (m/s), $\varepsilon_{\max}$ is the maximum volume tensile strain rate (dimensionless).

The calculation of the average radius of micro-cracks in the formula does not take into account the dynamic impact of rock under repeated discharge impact, which is inconsistent with the actual situation.

In order to overcome the shortcomings of the above calculation methods, better describe the dynamic influence of repeated discharge on rock fatigue damage and failure, and accurately characterize the dynamic hange of rock micro-crack radius, this paper introduces the normal relative displacement as the crack width and proposes a correction formula that can not only truly reflect the dynamic hange of rock micro-cracks but also considers the influence of different discharge energy and discharge times on it.

3.1.1. Rock Micro-Crack Cracking Degree

The process of shock wave damage to rock is a transformation process from continuous to discontinuous. In the process of action, the structure of the material is damaged and destroyed, resulting in crack initiation and propagation and changes in the mechanical properties of the crack tip region. The cohesive zone model is usually used to describe the mechanical properties of the crack tip region [26].

As shown in Figure 1a, the rock will open normally when the micro-cracks are formed. As shown in Figure 1b, with the increase in the number of repeated discharges, the tensile strength of the rock gradually decreases. Under different loading conditions, with the increase in the number of discharges, the reduction of the tensile strength of rock due to damage varies.

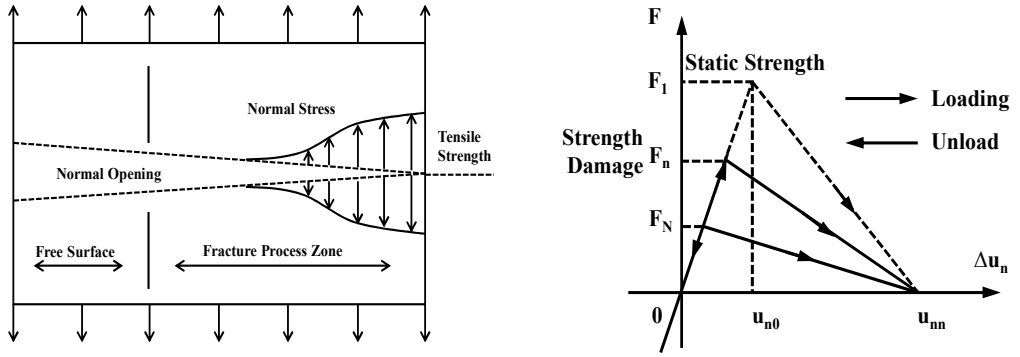

(**a**) (**b**)

Figure 1. Rock damage model; (**a**) Cohesive crack model; (**b**) Rock Fatigue Damage Stress Curve.

The cohesion model is used to describe the tensile mechanical properties of cracks, and to characterize the deterioration degree of the tensile strength of rock samples.

$$G'_{ff} = \frac{1}{2} F_n u_{nn} \tag{10}$$

The ultimate displacement u_{nn} when the normal opening displacement of the crack reaches failure can be obtained by the tensile fracture energy.

$$F_n(t_1) = -F_n^2 \Delta u_n / \left(2G'_{ff}\right) + F_n \tag{11}$$

where $F_n(t_1)$ is the interfacial tensile strength after the next impact (MPa), Δu_n is the normal relative displacement on the interface (mm), G'_{ff} it is tensile fracture energy (MPa).

3.1.2. Tensile Strength Attenuation Formula

The tensile strength attenuation model needs to meet the boundary conditions:

$$\left.\begin{array}{l} F(0) = F_0 \\ F(N) = F_t \\ \frac{dF(n)}{dn} \leq 0 \\ \frac{d^2F(n)}{dn^2} < 0 \end{array}\right\} \tag{12}$$

where $F(0)$ is the tensile strength of rock samples under hydrostatic pressure (MPa), $F(N)$ is the fatigue tensile strength of the sample when the number of shocks under shock wave loading is N (MPa).

The attenuation formula of damage tensile strength is established:

$$F(n) = F(0) - \left[F(0) - F_f\right] \tag{13}$$

where F_f is the fatigue tensile strength (MPa).

When the discharge impact is repeated, the fatigue tensile strength F_f of rock under different discharge times can be determined by hydraulic fracturing.

During hydraulic fracturing, the rock stress is redistributed due to the effect of water pressure around the borehole. When the hydraulic pressure reaches the fracture pressure of the rock, the rock fracture starts to crack and expand.

According to the maximum tensile stress criterion, when the maximum tensile stress of the rock reaches its tensile strength, the rock will undergo tensile failure [27]. Formula (14) is obtained.

$$F_f = 3\sigma_h - \sigma_H - M \tag{14}$$

where σ_h is the minimum principal stress (MPa), σ_H is the maximum principal stress (MPa), M is the original fracture pressure of rock (MPa).

However, due to the impact of discharge, the fatigue damage of rock accumulates continuously and the fracture pressure weakens gradually. Therefore, it is necessary to establish the rock fracture pressure weakening parameter formula under different discharge impact energy and discharge impact times.

3.2. Fracture Pressure Weakening

The weakening parameters of rock fracture pressure under the action of different discharge energy and discharge times are explored through experiments, and the calculation formula that can be expressed quantitatively is established.

3.2.1. Rock Samples

Select the sandstone outcrop of the Chang6 interval in the Yulin block of Yanchang Oilfield, as shown in Figure 2, and make a standard cylindrical core with a diameter of 25 mm and a height of 50 mm.

Figure 2. Standard sandstone core column.

3.2.2. Discharge Test Platform

All the discharge work involved in this study was completed on the self-developed discharge experimental platform. As shown in Figure 3a, the discharge platform is mainly composed of a pulse high-voltage power supply and a discharge chamber, which are connected by copper bars. The energy storage capacitance of the pulse high-voltage power supply is 50–250 μF, and the discharge voltage is 4–10 kV. The discharge chamber mainly consists of a water tank, discharge window, core holder, and discharge electrode. The core gripper is shown in Figure 3b.

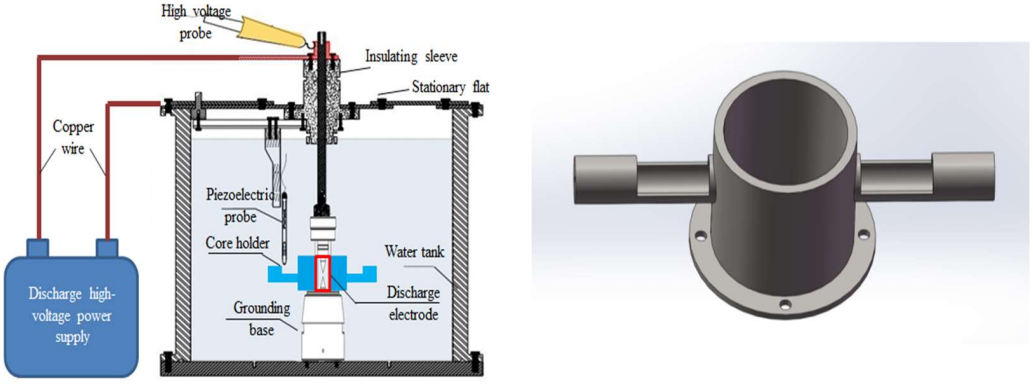

(**a**) (**b**)

Figure 3. Discharge platform and core holder; (**a**) Discharge platform; (**b**) Core holder.

3.2.3. Test Scheme

The test steps include four stages, test preparation, sample installation, discharge shock, and sample test.

Firstly, the processed rock samples were immersed in water for 72 h to meet the medium conditions of shock wave propagation inside the rock.

The second step is sample installation. Before the test, the rock sample was placed in the core holder, and the core holder is sheathed outside the discharge window. To achieve the purpose of monitoring the test process, the voltage probe was placed at the front end of the loaded core.

As shown in Figure 3a, water is injected into the discharge chamber to the no-overvoltage probe, then the fixed cover plate is covered and the high-voltage probe is connected.

In the process of the discharge impact stage, firstly, the capacitor capacitance is determined, the discharge voltage is adjusted, and the oscilloscope operation is monitored. Secondly, the discharge impact rock is started. Last, when the discharge times are divided into 20, 50, 100, 150, and 200 times, take out the samples, measure, and obtain the parameters of the acoustic wave velocity of the rock samples at different discharge stages.

Shock wave energy and discharge times are the main loading conditions for the fatigue damage and failure test of the rock caused by the shock wave. The discharge energy is regulated by capacitor capacitance and discharge voltage. Calculation of single discharge energy by Formula (15) [28].

$$E_b = \frac{1}{2} C U_0^2 \eta_0 \times 10^{-3} \tag{15}$$

where C is the capacitor capacitance in the discharge device (μF), U_0 is the initial discharge voltage (kV), η_0 is the efficiency of converting energy into action energy (%).

The major purpose of the experiment is to explore the weakening degree of rock mechanical parameters under different discharge energy and discharge times.

For this purpose, according to the loading conditions of the existing experimental equipment, four different sets of discharge test schemes with a discharge energy of 2.5 kJ, 5.0 kJ, 7.5 kJ, and 10 kJ are designed, respectively, and the discharge times of each set of discharge schemes are 20, 50, 100, 150 and 200, respectively (rock acoustic wave and other parameters are tested at each stage).

3.2.4. Variation of Rock Mechanical Properties

The purpose of this paper is to explore the impact of repeated shock wave action on the fatigue damage and failure of rock from the point of view of weakening the compressive strength of rock through the uniaxial static compression capacity test.

The average uniaxial compressive strength of the tested rock is 68.48 MPa. Limited by the limit of irreversible damage to rock caused by the uniaxial static load compression test, this paper uses the characteristics of acoustic velocity change to explore rock damage and its cumulative effect. The experimental results are shown in Table 1.

The test results show that after the action of discharge shock wave, the permeability of rock increases and the acoustic wave velocity decreases, indicating that the rock is damaged, the integrity is deteriorated, and the rigidity is weakened. However, the weakening degree of its mechanical properties needs to be calculated and deduced by a formula.

Table 1. Physical properties of rock and results of uniaxial static compressive test.

No.	Porosity before Discharge/(%)	Porosity after Discharge/(%)	Permeability before Discharge/(mD)	Permeability after Discharge/(mD)	Longitudinal Wave Velocity before Discharge/(m/s)	Longitudinal Wave Velocity after Discharge/(m/s)	Compressive Strength/(MPa)	Young's Modulus/(MPa)	Poisson Ratio
1	16.48	18.2	61.18	66.3	3266.80	2642.15	68.1	8619.1	0.22
2	16.47	18.1	67.58	79.3	3213.14	2538.62	61.8	9614.5	0.23
3	16.1	18.5	68.31	77.7	3213.37	2276.51	51.6	7683.32	0.23
4	16.21	18.9	65.55	143	3186.18	2196.84	40.4	9244.57	0.23

3.2.5. Quantitative Characterization of Shock Wave Effect

Theory and practice show that rock damage can be reflected by the change in rock sound velocity. It is an effective method to explore rock damage and its cumulative effect by using the change characteristics of sound velocity [29–31]. This is because, with the crease of the number of discharge shocks, new damage is continuously generated inside the rock, and the sound wave is constantly refracted and reflected during the transmission process inside the rock, resulting in the loss of sound wave energy, the extension of the propagation path, and finally the reduction of the sound wave speed. Therefore, before the deformation degree of rock reaches the limit, the damage degree can be used to reveal the damage and accumulation process by using the acoustic wave characteristics of rock [32,33].

The mechanical parameters of rock are calculated according to the Hoek–Brown empirical criterion [34].

$$\sigma_H = \sigma_h + \sqrt{m_b \sigma_{ci} \sigma_h + s\sigma_{ci}^2} \tag{16}$$

where σ_{ci} is the uniaxial compressive strength of intact rock (MPa), m_b is the Hoke Brown constant of rock (dimensionless), s is the constant related to rock quality and reflects the degree of rock fragmentation (dimensionless).

The rock compressive strength values at different discharge energies and discharge times are obtained by acoustic wave tests. As shown in Table 2.

Table 2. Changes of rock compressive strength and tensile strength under different discharge times.

Discharge Energy/(kJ)	Discharge Times	Rock Compressive Strength/(MPa)	Uniaxial Test Results/(MPa)	Tension Strength of Rock/(MPa)
2.5	20	69.68	68.1	23.5
	50	69.20		23.1
	100	69.33		22.6
	150	68.41		22.3
	200	68.89		21.7
5.0	20	66.79	64.8	19.3
	50	65.01		18.7
	100	63.90		18.4
	150	62.17		18.2
	200	64.03		17.9
7.5	20	66.07	51.6	16.2
	50	63.26		15.5
	100	58.78		15.2
	150	54.61		14.4
	200	50.74		13.7
10	20	64.74	40.4	12.7
	50	60.08		11.3
	100	52.88		10.6
	150	46.54		10.1
	200	40.96		9.6

Considering that each discharge impact will cause damage to the rock and affect the effect of the next energy, the impact energy formula can be established.

$$rE_b^t = (M - M_n)/n \tag{17}$$

where M_n is the compressive strength of rock after n times of discharge (MPa), r is a constant 0.0001 (dimensionless), t is the attenuation coefficient of shock wave energy under different conditions (dimensionless), $t = \begin{cases} 1.89 & E_b < 5 \\ 1.48 & E_b \geq 5 \end{cases}$.

In this paper, the compressive strength of rock is used as the mechanical characterization parameter of rock effect under shock waves. Combined with Formulas (16) and (17), the weakening parameter Pm of rock compressive strength under shock wave is obtained:

$$P_m = n \times M \times r \times E_b^t \tag{18}$$

Formulas (14) and (18) are established to calculate the fatigue tensile strength of rock.

$$F_f = 3\sigma_h - \sigma_H - M + P_m \tag{19}$$

Based on the above derivation, the final modified model obtained from the simultaneous formula is follows:

$$\sigma(n) = E\left(1 - \frac{16}{9}\frac{(1-\overline{v}^2)}{(1-2\overline{v})}\beta k\varepsilon^m(\Delta u_n)^3\right)\varepsilon(n) \tag{20}$$

In the process of repeated impact, the degree of rock damage gradually increases, the mechanical parameters continue to deteriorate, and new cracks gradually appear inside the body. Therefore, the fatigue damage process of rock is the dynamic change process of micro-cracks with the hange of discharge energy and discharge times, and the density of cracks formed eventually affects the stress hange of the rock.

3.3. Example Analysis

Based on the test rock sample parameters (Table 3), the corresponding calculation results are obtained by modifying the model calculation Formula (20) as shown in Figure 4.

Table 3. Basic calculation parameters.

Parameter	σ_h/(MPa)	σ_H/(MPa)	M/(MPa)	E/(MPa)	β	m	v
numerical value	21	24	22	18	3	6	0.24

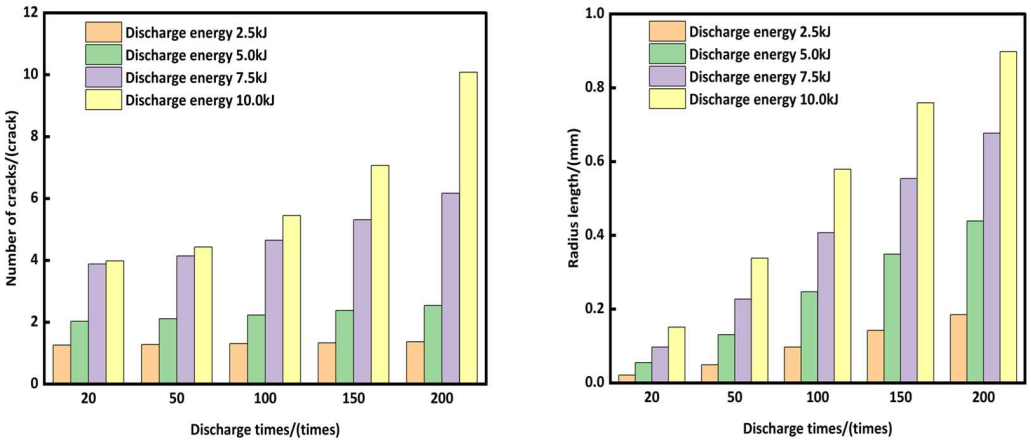

(**a**) (**b**)

Figure 4. *Cont.*

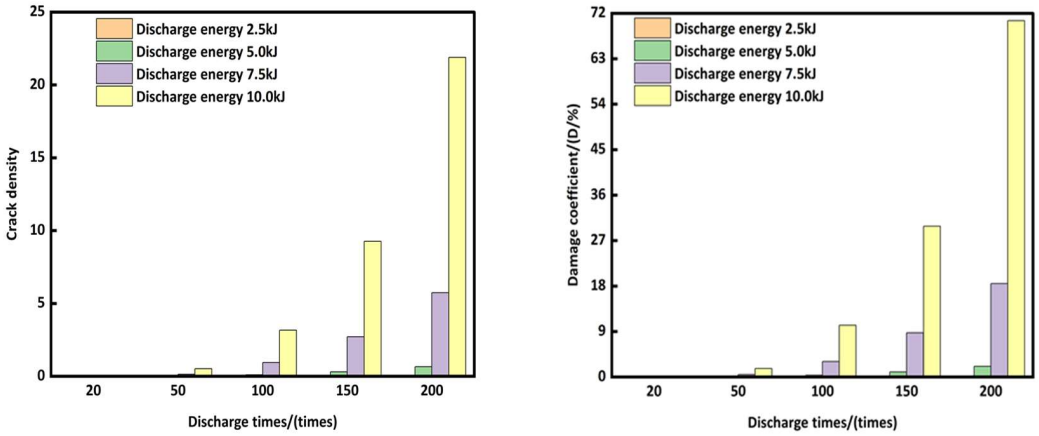

(**c**) (**d**)

Figure 4. Effect of different discharge energy and times on rock samples; (**a**) Number of cracks N change; (**b**) hange of crack radius length α; (**c**) hange of crack density C_d; (**d**) hange of damage coefficient D.

Figure 4 shows that when the discharge energy is greater than 5.0 kJ and the number of discharges is less than 200 times, the discharge energy has little effect on the number of cracks caused by rock fatigue damage. However, when the discharge energy reaches 200 times, the shock wave has a significant damage effect on the rock sample. It can be seen from Figure 4b that the crack radius length increases with the crease of discharge energy and discharge times. It can be seen from Figure 4c,d that when the number of discharges is less than 100 times, the damage of the shock wave load to the rock is not obvious. When the number of discharges reaches 150 times, it has a relatively obvious effect on the rock.

4. Simulation and Verification

The above test and model calculation results show that the repeated discharge shock waves can damage the rock through fatigue damage and generate cracks. Simulation is effective in the study of crack propagation [35,36]. To verify the modified model and better explore the effect of repeated discharge shock waves on rock fatigue damage, this paper further carried out simulation research.

4.1. Simulation Model Establishment

4.1.1. Modelling

The ANSYS-AUTODYN model is used to simulate the fatigue damage of rock under discharge impact. The boundary conditions, mechanical parameters, and related simulation parameters of the calculation model are consistent with the test materials and test conditions. The model is shown in Figure 5. To establish the shock wave transmission channel, a penetration seam is preset inside the simulation model. The model involves the interaction of underwater explosion load, rock, and medium water. Therefore, in the equivalent simulation, the Euler and ALE algorithms are used for fluid materials [37], and the lagrangian algorithm is used for other structures, and the interaction is processed by fluid-solid coupling [36].

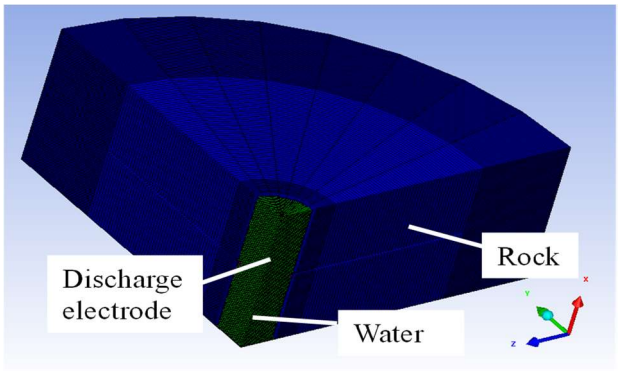

Figure 5. Simulation model establishment.

4.1.2. Discharge Shock Wave Energy Equivalent

TNT explosive is usually used as impact power source in the AUTODYD program. The TNT explosive state equation in the model is described by the standard JWL state equation [37], and the specific form is Formula (21).

$$p = A\left(1 - \frac{\omega}{R_1 V}\right)e^{-R_1 V} + B\left(1 - \frac{\omega}{R_2 V}\right)e^{-R_2 V} + \frac{\omega E_i}{V} \tag{21}$$

where p is the pressure of detonation products, E_i is the internal energy per unit volume, V is the specific volume, that is the volume of detonation products produced by unit volume charge, A, B, R_1, R_2, and ω are the parameters of JWL state equation. The specific parameters are, density ρ = 1.630 kg/cm^3, C-J detonation pressure p_{CJ} = 27 GPa, A = 374 GPa, B = 7.33 GPa, R_1 = 4.15, R_2 = 0.95, ω = 0.3, E_i = 7 GJ/m^3 [36].

Different from the equivalence of explosion energy, the equivalence of shock wave energy is mainly based on the equivalence of shock wave energy generated by the explosion and shock wave energy generated by the electrohydraulic effect. The specific expressions are as follows:

$$E_w = \frac{m_T}{0.24 \times 10^{-3}} \tag{22}$$

where E_w is the shock wave energy generated by the electrohydraulic effect, and the right end term is the shock wave energy generated by the explosion, kJ.

The designed discharge energies are 2.5 kJ, 5.0 kJ, 7.5 kJ, and 10.0 kJ, respectively. The mass fractions of TNT explosives are 0.6 g, 1.2 g, 1.8 g, and 2.4 g.

4.2. Analysis of Simulation Results

Figure 6 shows the actual experimental results and the results of electron microscopy scanning image processing. Table 4 shows the micro-crack widths of different rock samples in Figure 6. The pictures in Table 5 are the crack initiation and distribution characteristics of the model under the discharge energy conditions of 2.5 kJ, 5.0 kJ, 7.5 kJ, and 10.0 kJ, and discharge times of 20, 50, 100, 150, and 200 times. In the damage degree bar, different colors indicate the degree of damage to the rock material, in which blue is no damage and red is complete damage.

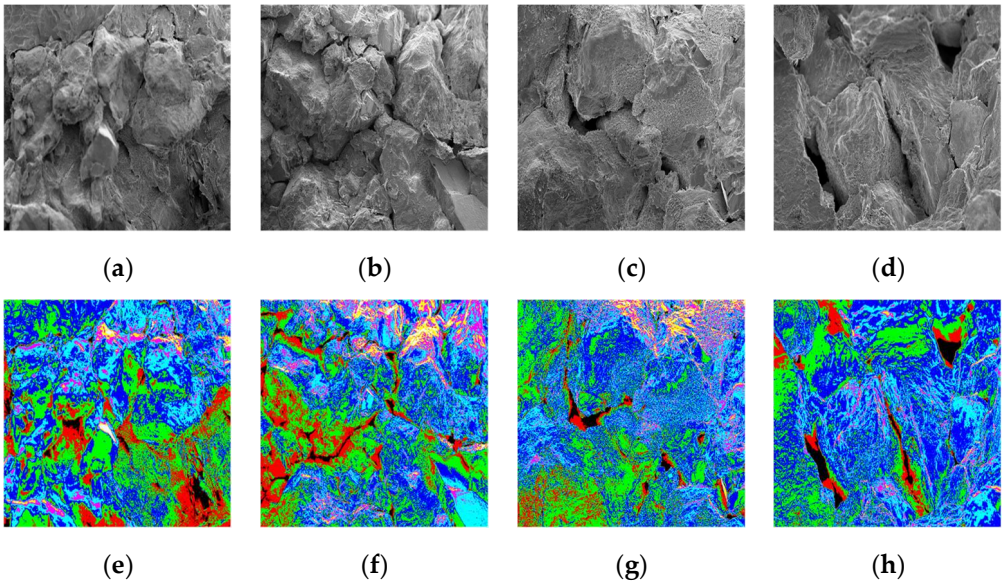

Figure 6. Scanning electron microscopy results and colorization processing of grayscale images (**a**) Discharge times 200, discharge energy 2.5 kJ; (**b**) Discharge times 200, discharge energy 5.0 kJ; (**c**) Discharge times 200, discharge energy 7.5 kJ; (**d**) Discharge times 200, discharge energy 10 kJ; (**e**) After color processing: Discharge times 200, discharge energy 2.5 kJ; (**f**) After color processing: Discharge times 200, discharge energy 5.0 kJ; (**g**) After color processing: Discharge times 200, discharge energy 7.5 kJ; (**h**) After color processing: Discharge times 200, discharge energy 10 kJ.

Table 4. Micro-crack width.

Discharge Energy/(kJ)	Discharge Times	Roundness/(Round)	Micro-Crack Width/(μm)
2.5	200	0.761	207.57
5.0	200	0.463	403.38
7.5	200	0.549	750.62
10.0	200	0.742	1055.89

It can be seen from the Figure that:

- Under different discharge impact conditions, the crack initiation orientation of rock is basically the same, and the final parameters of crack are different due to the influence of discharge energy and discharge times.
- Under the same discharge energy condition, with the crease of discharge time, the crack length and width increase. However, when it increases to a certain extent, it will not continue to expand, but generate new cracks, indicating that the increase of discharge times is helpful to form new cracks.
- Under the same discharge times, with the crease of discharge energy, the crack initiation time in the model is earlier, the crack length is longer, and the width is wider, indicating that the higher the discharge energy, the more serious the rock damage and failure effect.
- When the discharge energy is less than or equal to 5.0 kJ, the increase of the number of discharges does not increase the number of cracks, but extends the length of the generated cracks. When the discharge energy is greater than or equal to 7.5 kJ, the initial crack length and width increase to a certain extent, and new cracks will be generated.
- The crack growth presents a staged pattern, with discharge times of 0–50 times in the crack initiation state, 50–150 times in the crack rapid extension state, and 150–200 times

in the original crack reaching the extension limit, which is accompanied by the formation of some new cracks.

4.3. Comparison of Calculation Results

In the AUTODYN calculation results file, the model crack parameters are measured by adjusting the View range option and the Axes attachment. The comparison between the simulation results and the modified model calculation results is shown in Table 5.

Table 5. Development of rock cracks under different loads and impacts.

Discharge Energy	20	50	100	150	200
2.5 kJ	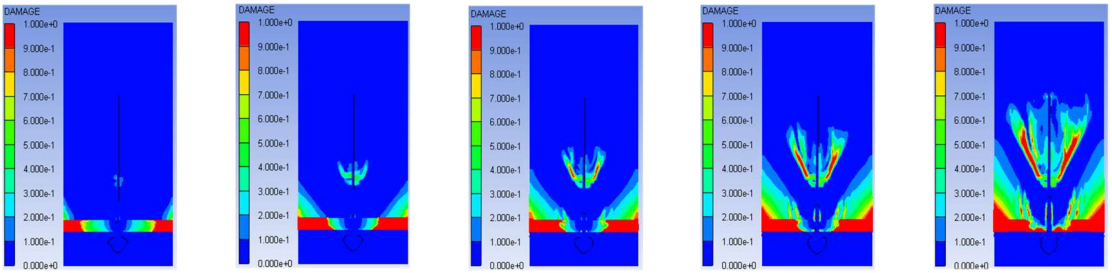				
5.0 kJ	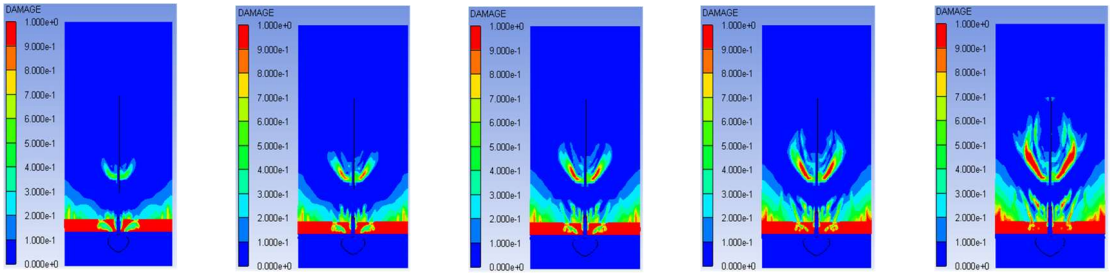				
7.5 kJ	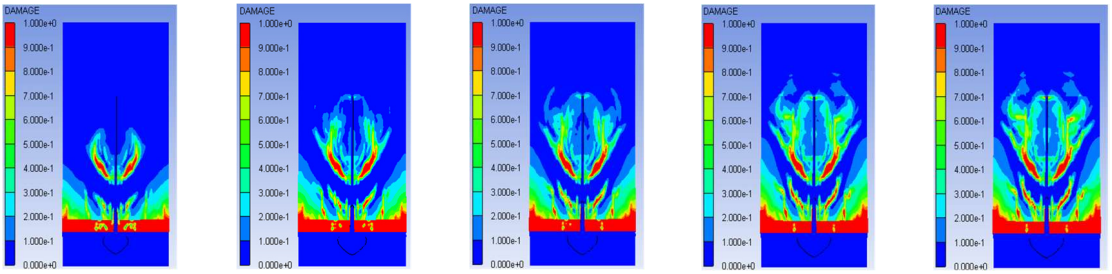				
10.0 kJ	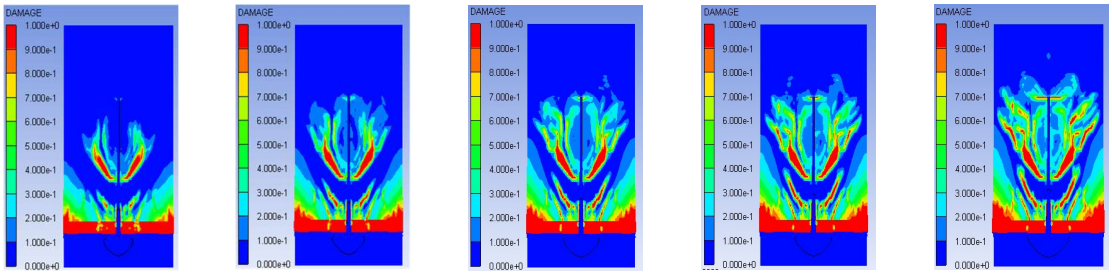				

The results show that the error between the calculated results of the modified TCK model and the simulation results of the simulation software is 0.8–16.8%, with an average of 7.14% and 8.15%, respectively (Table 6). The two are consistent, confirming the correctness of the modified model.

Table 6. Comparison of simulation results and modified model calculation results.

Discharge Energy (kJ)	Discharge Times/(n)	Corrected Model Calculation Crack Number N/(Crack)	Number of Cracks in Simulation Result N/(Crack)	Error/(%)	Corrected Model Calculation Crack Radius A/(mm)	Simulation Results Crack Radius A/(mm)	Error/(%)
2.5	20	1.26	0	/	0.021	0	/
	50	1.28	0.32	12.5	0.049	0	/
	100	1.31	0.5	2	0.097	0.113	14.2
	150	1.33	1.5	11.3	0.142	0.165	13.9
	200	1.37	2	11.5	0.185	0.213	13.1
5	20	2.03	1	3	0.055	0	/
	50	2.11	2	5.5	0.131	0.1575	16.8
	100	2.23	2	11.5	0.247	0.25	1.2
	150	2.38	2.1	13.3	0.349	0.388	10.1
	200	2.54	2.6	2.3	0.439	0.45	2.4
7.5	20	3.88	4	3	0.097	0.115	15.7
	50	4.14	4	3.5	0.227	0.257	11.7
	100	4.65	4	16.3	0.407	0.387	5.1
	150	5.31	6	11.5	0.554	0.636	12.9
	200	6.17	6	2.8	0.677	0.726	6.7
10	20	3.98	4	0.5	0.151	0.163	7.4
	50	4.43	4	10.8	0.338	0.374	9.6
	100	5.45	6	9.2	0.579	0.577	0.3
	150	7.07	8	11.6	0.759	0.7	8.4
	200	10.08	10	0.8	0.898	1.03	12.8

5. Conclusions

In order to explore the fatigue-damage effect of repeated discharge shock wave on rock. Based on the test, this paper establishes the calculation formula for weakening the mechanical properties of rock by using different discharge parameters and also establishes sets up the correction formula of the TCK model from the perspective of dynamic damage. Finally, the accuracy of the model is verified by numerical simulation, and the effects of different discharge impact parameters on rock is deeply compared and analyzed.

The main conclusions are as follows.

1. Under the action of the discharge shock wave, the rock has micro-cracks. The higher the discharge energy and the more the number of times, the greater the tensile stress value generated at the crack tip, and the easier the crack is to crack. This shows that the method of repeated discharge impact fatigue damage to rock is effective and technically feasible, and the higher the discharge energy and the number of times, the better the damage effect.
2. Considering rock failure damage and its fatigue effect, this paper points out the deficiency of dynamic damage calculation of TCK model criteria under repeated discharge, characterizes rock damage factor D in the way of the weakening degree of rock mechanical properties; and establishes a correction method that can truly and quantitatively reflect rock fatigue damage effect, micro-crack formation state, and the weakening degree of mechanical parameters under different discharge energy and discharge times.
3. The results of the modified model are verified by establishing a simulation model that is consistent with the test materials and test conditions, and the results are basically consistent, confirming that the modified model is correct and feasible. At the same time, the simulation results show that the crack initiation time of high discharge energy is earlier, the number of cracks is more, the crack opening is longer, and the width is wider than that of low discharge energy under the same discharge times. Under the same discharge energy, with the crease of discharge times, new cracks will continue to form around the micro-cracks after they open to the limit value, until the rock is completely destroyed.
4. The proposed model plays a significant role in advancing the application of discharge impact technology in the field of oil and gas reservoir development. It enables the rapid selection of discharge impact energy and frequency for different sandstone reservoir characteristics, leading to the most cost-effective and optimized reformation outcomes.

Author Contributions: C.L.: conceptualization, methodology, supervision, funding acquisition, writing—review & editing; X.L.: methodology, validation, writing—original draft, investigation, writing—review & editing; J.G.: supervision, funding acquisition; S.X.: methodology, validation. X.L. and X.Z. and K.H.: experiment, writing—review & editing; S.X. and X.Z.: review & editing. All authors have read and agreed to the published version of the manuscript.

Funding: This research was funded by the National Natural Science Foundation of China Joint Fund Project Key Support Project (grant number U21A20105) and Sichuan Provincial Applied Basic Research Program Project "Optimization and Improvement of Shale Gas Production by Pulse Discharge Shock Wave Stimulation Technology" (No. 2022NSFSC1261) and National Natural Science Foundation (52022087) and Sichuan Provincial Science and Tech-nology Plan Project (2023JDRC0008).

Data Availability Statement: Data are available in the article.

Acknowledgments: All individuals included in this section have consented to the acknowledgement.

Conflicts of Interest: The authors declare no conflict of interest.

Nomenclature

σ	the stress in tensor form (MPa)
ε	the volume strain (dimensionless)
E	elastic modulus (MPa)
D	the damage variable (dimensionless)
n	the number of discharges (time)
K, K	the bulk modulus (MPa)
$\overline{v}$	effective Poisson's ratio (dimensionless)
C_d	micro-crack density (quantity/cm^2)
β	coefficient (dimensionless)
N	the number of cracks activated by rock impact (quantity)
α	the average radius of micro-cracks (mm)
k, m	rock parameters in damage model (dimensionless)
Ω	the damage tensor of jointed rock mass (MPa)
l	the average crack spacing (mm)
V	the sample volume (mm^3)
α_k	the surface area of the k-th crack in the sample (mm^2)
n_k	the unit normal vector on the surface of the k-th crack in the sample (dimensionless)
K_{IC}	fracture toughness (MPa)
ρ	density (kg/m^3)
C_P	longitudinal wave velocity (m/s)
$\varepsilon_{\max}$	the maximum volume tensile strain rate (dimensionless)
u_{nn}, Δu_n	the normal displacement (mm)
G''_{ff}	the tensile fracture energy (MPa)
F_n, F_f	tensile strength (MPa)
$F_n(t1)$	the interfacial tensile strength after the next impact
$F(0)$	the tensile strength of rock samples under hydrostatic pressure (MPa)
$F(N)$, $F(n)$	the fatigue tensile strength of the sample when the number of shocks under shock wave loading is N/n (MPa)
σ_h	minimum horizontal principal stress (MPa)
σ_H	maximum horizontal principal stress (MPa)
σ_{ci}	the uniaxial compressive strength of intact rock (MPa)
M	compressive strength (MPa)
M_n	the compressive strength of rock after n times of discharge (MPa)
E_b	discharge energy (kJ)
C	the capacitor capacitance in the discharge device (μF)
U_0	the initial discharge voltage (kV)
η_0	the efficiency of converting energy into action energy (%)
m_b	the Hoke-Brown constant of rock (dimensionless)
s	constant (dimensionless)
r	a constant (dimensionless)
t	the attenuation coefficient of shock wave energy (dimensionless)
P_m	the reduction value of rock compressive strength after n discharge (MPa)

References

1. Wu, Q.; Xu, Y.; Zhang, L.; Wang, T.; Guan, B.; Wu, G.; Wang, X. Core theory and key to optimal design of unconventional reservoir volume transformation technology. *J. Pet.* **2014**, *35*, 706–714.
2. Wu, Q.; Xu, Y.; Wang, T.; Wang, X. A major change in the concept of increasing production and Transformation—Introduction to volume transformation technology. *Nat. Gas Ind.* **2011**, *31*, 7–12, 16, 121–122.
3. Chen, Z.; Xue, C.; Jiang, Y.; Qin, Y. Application suggestions of shale gas well volume fracturing technology in China. *Nat. Gas Ind.* **2010**, *30*, 30–32, 116–117.
4. Peng, K.; Zhou, J.Q.; Zou, Q.L.; Song, X. Effect of loading frequency on the deformation behaviours of sandstones subjected to cyclic loads and its underlying mechanism. *Int. J. Fatigue* **2020**, *131*, 105349.1–105349.12.
5. Peng, K.; Zhou, J.; Zou, Q.; Zhang, J.; Wu, F. Effects of stress lower limit during cyclic loading and unloading on deformation characteristics of sandstones. *Constr. Build. Mater.* **2019**, *217*, 202–215.
6. Shi, Z.; Li, J.; Wang, J. Research on the fracture mode and damage evolution model of sandstone containing pre-existing crack under different stress paths. *Eng. Fract. Mech.* **2022**, *264*, 108299.

7. Wang, J.; Li, J.; Shi, Z. Deformation damage and acoustic emission characteristics of red sandstone under fatigue-creep interaction. *Theor. Appl. Fract. Mech.* **2021**, *117*, 103192. [CrossRef]
8. Liu, Y.; Dai, F. A review of experimental and theoretical research on the deformation and failure behavior of rocks subjected to cyclic loading. *J. Rock Mech. Geotech. Eng.* **2021**, *13*, 1203–1230. [CrossRef]
9. Ge, X.R.; Jiang, Y.; Lu, Y.D.; Ren, J.X. Testing study on fatigue deformation law of rock under cyclic loading. *J. Rock Mech. Eng.* **2003**, *22*, 1581–1585.
10. Zhou, Z.-L.; Wu, Z.-b.; Li, X.-b.; Li, X.; Ma, C.-d. Mechanical behavior of red sandstone under cyclic point loading. *Trans. Nonferrous Met. Soc. China* **2015**, *25*, 2708–2717.
11. Song, Z.; Konietzky, H.; Herbst, M. Three-dimensional particle model based numerical simulation on multi-level compressive cyclic loading of concrete. *Constr. Build. Mater.* **2019**, *225*, 661–677.
12. Song, Z.; Fruehwirt, T.; Konietzky, H. Inhomogeneous mechanical behaviour of concrete subjected to monotonic and cyclic loading. *Int. J. Fatigue* **2020**, *132*, 105383.1–105383.14.
13. Zhou, B.; Wang, J.H. Three-dimensional sphericity, roundness and fractal dimension of sand particles. *Geotechnique* **2018**, *68*, 18–30. [CrossRef]
14. Zhou, B.; Wei, D.; Quan, K.; Wang, J.; Zhang, A. Study on the effect of particle morphology on single particle breakage using a combined finite-discrete element method. *Comput. Geotech.* **2020**, *122*, 103532.
15. Li, D.; Zhu, Q.; Zhou, Z.; Li, X.; Ranjith, P.G. Fracture analysis of marble specimens with a hole under uniaxial compression by digital image correlation. *Eng. Fract. Mech.* **2017**, *183*, 109–124.
16. Wang, Y.; Tang, J.; Dai, Z.; Yi, T. Experimental study on mechanical properties and failure modes of low-strength rock samples containing different fissures under uniaxial compression. *Eng. Fract. Mech.* **2018**, *197*, 1–20.
17. Yang, S.Q.; Huang, Y.H.; Ranjith, P.G. Failure mechanical and acoustic behavior of brine saturated-sandstone containing two pre-existing flaws under different confining pressures. *Eng. Fract. Mech.* **2018**, *193*, 108–121.
18. Budiansky, B.; Connell, R.J. Elastic moduli of a cracked solid. *Int. J. Solids Struct.* **1976**, *12*, 81–97. [CrossRef]
19. Grady, D.E.; Kipp, M.E. Continuum modelling of explosive fracture in oil shale. *Int. J. Rock Mech. Min. Sci. Geomech. Abstr.* **1980**, *17*, 147–157. [CrossRef]
20. Taylor, L.M.; Chen, E.P.; Kuszmaul, J.S. Microcrack-induced damage accumulation in brittle rock under dynamic loading. *Comput. Methods Appl. Mech. Eng.* **1986**, *55*, 301–320. [CrossRef]
21. Zuo, Q.H.; Disilvestro, D.; Richter, J.D. A crack-mechanics based model for damage and plasticity of brittle materials under dynamic loading. *Int. J. Solids Struct.* **2010**, *47*, 2790–2798.
22. Zlw, A.; Ycl, A.; Jgw, B. A damage-softening statistical constitutive model considering rock residual strength-sciencedirect. *Comput. Geosci.* **2007**, *33*, 1–9.
23. Zhu, C.Y.; Yu, S.C. Study on the discriminance of rock mass damage induced by blasting. *Eng. Blasting* **2001**, *7*, 12–16.
24. Kyoya, T.; Ohashi, T.; Kawamoto, T. Damage mechanics analysis of underground opening in jointed rock mass. *J. Soc. Mater. Sci. Jpn.* **1986**, *35*, 472–477. [CrossRef]
25. Kawamoto, T.; Ichikawa, Y.; Kyoya, T. Deformation and fracturing behavior of discontinuous rock mass and damage mechanics theory. *Int. J. Numer. Anal. Method Geomech.* **1988**, *12*, 1–30.
26. Haeri, H. Experimental crack analyses of concrete-like cscbdspecimens using a higher order ddm. *Comput. Concr.* **2015**, *16*, 881–896.
27. Li, H. *Rock Fracture Mechanics*; Chongqing University Press: Chongqing, China, 1988.
28. Liu, Y.; Li, Z.; Li, X.; Zhou, G.; Li, H.; Zhang, Q. Energy transfer efficiency improvement of liquid pulsed current discharge by plasma channel length regulation method. *IEEE Trans. Plasma Sci.* **2017**, *45*, 3231–3239. [CrossRef]
29. Yan, C.B.; Xu, G.Y.; Yang, F. Measurement of Sound Waves to Study Cumulative Damage Effect on Surrounding Rock Under Blasting Load. *Chin. J. Geotech. Eng.* **2007**, *29*, 88–93.
30. Yan, C.; Wang, G.; Shi, S.; Xu, G.Y. Analysis of acoustic wave frequency spectrum characters of rock mass under blasting damage based on wavelet (packet) transformation. *Chin. J. Rock Mech. Eng.* **2010**, *29*, 1496–1502.
31. Yang, R.L.; Rocque, P.; Katsababis, P. Measurement and analysis of near-field blast vibration and damage. *Geotech. Geol. Eng.* **1994**, *12*, 169–182. [CrossRef]
32. Zhang, L.; Yue, Z.; Yang, Z.; Qi, J.; Liu, F. A displacement-based back-analysis method for rock mass modulus and horizontal in situ stress in tunneling—Illustrated with a case study. *Tunn. Undergr. Space Technol. Inc. Trenchless Technol. Res.* **2006**, *21*, 636–649. [CrossRef]
33. Tan, C.; Wang, R.; Ye, S.; Lei, W.; Sun, W. Numerical modelling estimation of the 'tectonic stress plane' (tsp) beneath topography with quasi-u-shaped valleys. *Int. J. Rock Mech. Min. Sci.* **2004**, *41*, 303–310.
34. Ishihara, K.; Towhata, I. Sand response to cyclic rotation of principal stress directions as induced by wave loads. *Soils Found.* **1983**, *23*, 11–26. [CrossRef] [PubMed]
35. Sun, C.; Wei, Y.; Zhou, Z. *The Application of Detonation Physics*; National Defence Industry Press: Beijing, China, 2001.

36. Dobratz, B.M. Properties of chemical explosives and explosive simulants. In *LLNL Explosive Handbook*; Lawrence Livermore National Lab. (LLNL): Livermore, CA, USA, 2018; Volume 51, pp. 339–340.
37. Ma, G.W.; An, X.M. Numerical simulation of blasting-induced rock fractures. *Int. J. Rock Mech. Min. Sci.* **2008**, *45*, 966–975. [CrossRef]